Effect of noise amplification during the transition to amplitude death in coupled thermoacoustic oscillators

Nevin Thomas, Sirshendu Mondal, Samadhan A. Pawar, and R. I. Sujith

Citation: Chaos **28**, 093116 (2018); doi: 10.1063/1.5040561
View online: https://doi.org/10.1063/1.5040561
View Table of Contents: http://aip.scitation.org/toc/cha/28/9
Published by the American Institute of Physics

Effect of noise amplification during the transition to amplitude death in coupled thermoacoustic oscillators

Nevin Thomas,[1] Sirshendu Mondal,[2,a)] Samadhan A. Pawar,[1] and R. I. Sujith[1]
[1]*Department of Aerospace Engineering, Indian Institute of Technology Madras, Chennai 600036, India*
[2]*Department of Mechanical Engineering, Amrita Vishwa Vidyapeetham, Amritapuri, Kollam, 690525, India*

(Received 18 May 2018; accepted 6 September 2018; published online 26 September 2018)

We present a systematic investigation of the effect of external noise on the dynamics of a system of two coupled prototypical thermoacoustic oscillators, horizontal Rijke tubes, using a mathematical model. We focus on the possibility of amplitude death (AD), which is observed in the deterministic model of coupled thermoacoustic oscillators as studied by Thomas *et al.* [Chaos **28**, 033119 (2018)], in the presence of noise. Although a complete cessation of oscillations or AD is not possible in the stochastic case, we observe a significant reduction in the amplitude of coupled limit cycle oscillations (LCOs) with the application of strong coupling. Furthermore, as we increase the noise intensity, a sudden drop in the amplitude of pressure oscillations at the transition from LCO to AD, observed in the noise free case, is no longer discernible because of the amplification of noise in AD state. During this transition from LCO to AD, we notice a qualitative change in the distribution of the pressure amplitude from bimodal to unimodal. Furthermore, in order to demarcate the boundary of the transition from LCO and AD in the noisy case, we use 80% suppression in the amplitude of LCO, which generally occurs in the parameter range over which this qualitative change in the pressure distribution happens, as a threshold. With the help of bifurcation diagrams, we show a qualitative change as well as a reduction in the size of amplitude suppression zones that happen due to the increase in noise intensity. We also observe the relative ease of suppressing the amplitude of LCO with time-delay coupling when detuning and dissipative couplings are introduced between the two thermoacoustic oscillators in the presence of noise. *Published by AIP Publishing.* https://doi.org/10.1063/1.5040561

Practical combustors involved in most of the propulsive systems and power generation units are prone to thermoacoustic instabilities. Thermoacoustic instability is a consequence of the establishment of a positive feedback loop between the acoustic field and the unsteady heat release rate in a combustor, which leads to high amplitude pressure oscillations. These oscillations can have adverse effects on the life as well as performance of engines, and hence, the occurrence of such instabilities need to be controlled. Here, we study an approach based on coupling two thermoacoustic systems to suppress these unwanted thermoacoustic oscillations. Previous studies[1,2] have shown that AD or a complete cessation of oscillations is possible in such a scenario if the system dynamics is completely deterministic. However, all practical thermoacoustic systems are often subjected to inherent random fluctuations from different sources. In this paper, we study the effect of noise on the coupled behaviour of a system of two thermoacoustic oscillators working in the regime of limit cycle oscillations. We observe that, although attaining a complete cessation of oscillations through coupling is very difficult in the presence of noise, we can still achieve a significant suppression in the amplitude of limit cycle oscillations by an appropriate choice of coupling parameters. We further note that it is easier to achieve suppression when a small detuning is introduced between two time-delay coupled noisy thermoacoustic oscillators. When a weak dissipative coupling is applied on this system, the amplitude suppression is achieved with even greater ease. Similar to the earlier studies on stochastic systems, we use histogram of pressure amplitude as a measure to identify the increasingly continuous transitions from LCO to AD in the presence of noise. With an increase in noise intensity, we observe a departure from the abrupt nature of the transition from LCO to AD due to the growth of fluctuations near the bifurcation point in the AD state. It is similar to a phenomenon of prebifurcation noise amplification[3] that happens for a single oscillator during the transition from steady state to LCO as the control parameter is changed. Further, a reduction in the size of amplitude suppression zones in the parameter planes, at higher values of noise intensity, is also observed.

I. INTRODUCTION

The effect of fluctuating environments or noise on the behavior of deterministic nonlinear systems has always been of interest in the scientific community. This is due to the fact that, more often than not, the deterministic descriptions are incapable of capturing the influence of inherent noise present in natural systems. For instance, convection in atmospheric layers, formation of sand dunes under winds, etc., are all phenomena caused by instabilities occurring in a noisy environment.[4] Therefore, several theoretical models are developed to study the effect of noise on the dynamics of

a)Electronic mail: sirshendumondal13@gmail.com

nonlinear systems, and in turn, better predict the system behavior.

The term noise induced transitions is often used to refer to the capability of external fluctuations to induce novel dynamical states and transitions in deterministic systems.[5] In addition to the trivial disorganizing effect, noise is also found to stabilize or destabilize the steady state of a system, as seen in many previous studies.[6,7] Noise also possesses the characteristic of amplification of its fluctuations in the vicinity of a bifurcation point, wherein the fluctuations grow as a result of the decrease in damping coefficients of the nonlinear system.[3] Such behaviour of the noise is referred to as prebifurcation noise amplification.[8] Since this phenomenon occurs just before the bifurcation to limit cycle oscillation (LCO), it has been studied as a precursor to bifurcation.[3,8] In contrast, in the present study, we observe an existence of noise amplification which happens after the bifurcation from LCO to noisy amplitude death (AD) state in a system of coupled thermoacoustic oscillators.

As can be seen from the literature, coupling can give rise to phenomena such as synchronization and oscillation quenching in self-sustained nonlinear oscillators, depending on the dynamics of the system and the type and strength of the coupling.[9] Generally, weak coupling leads to synchronization or phase locking,[10,11] while strong coupling will affect the amplitude of oscillations resulting in phenomena such as oscillation quenching.[12,13] Amplitude death (AD) is one of the two structurally different manifestations of oscillation quenching (the other being oscillation death), wherein the oscillations of the individual oscillators cease completely and a stabilization to the fixed point of the system occurs.[14] We study the possibility of occurrence of AD or a considerable suppression of the amplitude of LCO when two thermoacoustic oscillators are coupled in the environment of noise.

In the present study, we numerically simulate the influence of external noise on the dynamics of two coupled prototypical thermoacoustic oscillators using a mathematical model. In simple terms, a thermoacoustic system is a duct with a heat source confined in it. When the acoustic pressure fluctuations in the duct are in phase with the heat release rate fluctuations, the acoustic field in the system amplifies and saturates to a state of large amplitude periodic oscillations called thermoacoustic instability.[15] Such instabilities are observed in a wide range of combustion systems including high performance propulsive systems such as rockets and aircraft engines, and power generation units such as land based gas turbine engines and boilers.[16–18] In addition to the adverse effects such as flame flashback and blowout,[19] the high amplitude oscillations that occur during thermoacoustic instability have the potential to cause structural damage and reduced performances of the engines and the control systems.[20] Recently, several efforts have been made to gain a deeper insight of the phenomenon using synchronization theory.[21–25] Further, given these adverse effects, the prediction and control of such instabilities are of great importance in real engines.[26,27]

Over the years, many passive[20,28] and active[17,29,30] methodologies have been developed to suppress the high amplitude pressure oscillations that are observed during thermoacoustic instabilities. Most of the passive approaches work well only over a limited range of operating conditions. On the other hand, active control approaches require complicated electro-mechanical feedback systems, limiting their practical applicability in real life gas turbine engines.[31] Relatively, newer strategies for damping these thermoacoustic oscillations include the use of external periodic forcing[32] and coupling of two thermoacoustic systems.[1,2] The difficulty in installing actuators with large control authority in real combustors, however, makes the approach based on external forcing practically challenging to implement. On the other hand, the methodology based on coupling of two or more thermoacoustic systems exhibiting limit cycle oscillations is relatively simpler. Recently, Thomas *et al.*[2] have used this coupling strategy and showed the possibility of achieving complete suppression of limit cycle oscillations in a deterministic model of two coupled thermoacoustic oscillators.

However, a complete cessation of oscillations is farfetched in practical systems. All such thermoacoustic systems are subjected to inherent noisy fluctuations from different sources such as combustion processes and incoming turbulent flows.[33] Furthermore, it has been hypothesized in the past that the sources of these turbulent fluctuations can be represented as additive[34] and parametric[35,36] noise. The effect of different kinds of noise (white, pink, blue, etc.) on the dynamics of an individual thermoacoustic oscillator has been studied in the past.[33,37] In the present study, we use coupled thermoacoustic oscillators and restrict ourselves to white noise. White noise is a random signal with a constant power spectral density, i.e., the energy is equally distributed among all the frequencies. We add white noise separately to the two individual self-sustained thermoacoustic oscillators, which are then coupled to achieve amplitude suppression in both the oscillators. Such suppression of thermoacoustic instabilities in coupled thermoacoustic oscillators is not a much explored field, but has significance in practice. However, complete cessation or AD in coupled thermoacoustic oscillators may not be possible in reality due to the presence of noise in the system. Therefore, a study on the effect of noise on the dynamics of coupled thermoacoustic oscillators needs to be performed.

To that end, we add white noise to the pre-existing model of the two Rijke tube systems coupled through dissipative and time-delay coupling.[2] While in the deterministic case, a complete cessation of oscillations or AD is possible with suitable coupling, the amplitude of oscillations does not go to zero in the presence of noise. However, we still get a considerable suppression under the appropriate coupling conditions. As the transition in the presence of noise lacks a clear cut indication of the occurrence of AD, we make use of the qualitative change in distribution of pressure amplitudes, as shown by histograms, towards this purpose. The change in the distribution from bimodal to unimodal demarcates the bifurcation from LCO to AD in the noisy case. However, since this change in the pressure distribution happens over a range of parameter values over which 80% suppression in the amplitude of LCO generally occurs, we use this level of suppression as the threshold. Further, from one-parameter bifurcation diagrams we observe that, with increase in the noise intensity, the abruptness of transitions from LCO to AD diminishes due

to the post bifurcation growth of noisy fluctuations in the AD state. We also observe the reduction in the size of amplitude suppression zones with noise intensity in the two-parameter bifurcation diagrams. In addition to this, these plots demonstrate the fact that, in the noise case also, it is easier to achieve amplitude suppression when the non-identical thermoacoustic oscillators are coupled simultaneous with the time-delay and dissipative coupling mechanisms.

II. MODEL FOR COUPLED RIJKE TUBE OSCILLATORS

We use a prototypical thermoacoustic system known as horizontal Rijke tube to conduct our study. A typical Rijke tube oscillator consists of a horizontal duct with a concentrated heat source (here, a heated cylinder). The analytical tractability offered by a Rijke tube oscillator has very often made it a preferred candidate for studying thermoacoustic instabilities in the past.[27,38–40]

The mathematical model developed by Balasubramanian and Sujith[39] for a single Rijke tube oscillator is used as the reference for the current study. A detailed explanation of modeling the coupling of two such Rijke tube oscillators can be found in the work by Thomas *et al.*,[2] where the study has been performed on a deterministic system. In this model, the linearized momentum and energy equations are solved to obtain the acoustic field in the duct by neglecting the effects of mean flow and mean temperature gradient. These equations are then non-dimensionalized, and an acoustic damping term[41] is added. Thus, we obtain a set of partial differential equations (PDEs), which govern the dynamics of the thermoacoustic system. Further, we use Galerkin technique to reduce the PDEs to a set of ordinary differential equations (ODEs). This is done by writing the acoustic pressure and velocity fluctuations in terms of basis functions, as shown in Eqs. (1) and (2). These basis functions are nothing but the natural acoustic modes of the duct in the absence of heat release rate oscillations.

$$u' = \sum_{j=1}^{N} \eta_j \cos(j\pi x), \tag{1}$$

$$p' = -\sum_{j=1}^{N} \dot{\eta}_j \frac{\gamma M}{j\pi} \sin(j\pi x). \tag{2}$$

Finally, after adding the coupling terms and the stochastic component, the temporal evolution of one of the Rijke tube oscillator can be obtained as follows:

$$\frac{d\eta_j^a}{dt} = \dot{\eta}_j^a, \tag{3}$$

$$\begin{aligned}\frac{d\dot{\eta}_j^a}{dt} + 2\zeta_j\omega_j\dot{\eta}_j^a + \omega_j^2\eta_j^a \\ = -j\pi K^a \left[\sqrt{\left|\frac{1}{3} + u_f'^a(t-\tau_1)\right|} - \sqrt{\frac{1}{3}}\right] \sin(j\pi x_f) \\ + \underbrace{\mathcal{K}_d(\dot{\eta}_j^b - \dot{\eta}_j^a)}_{\text{Dissipative coupling}} + \underbrace{\mathcal{K}_\tau(\dot{\eta}_j^b(t-\tau) - \dot{\eta}_j^a(t))}_{\text{Time-delay coupling}} + \underbrace{\sigma\epsilon(t)}_{\text{Noise}}.\end{aligned} \tag{4}$$

Here, the superscripts a and b correspond to the two Rijke tube oscillators. The subscript j refers to the j^{th} Galerkin mode. The variables, η_j and $\dot{\eta}_j$ are, respectively, the time-varying coefficients of the acoustic velocity (u') and acoustic pressure (p') in the Galerkin expansion, t is the time, ζ is the damping coefficient, x_f is the heater location along the duct, u_f' is the acoustic velocity at x_f, $\mathcal{K}_d$ is the dissipative coupling constant, and $\mathcal{K}_\tau$ is the time-delay coupling constant. While thermal inertia of the heat transfer in the medium is captured by the time lag τ_1, the delay associated with the time-delay coupling is represented by τ. All the variables mentioned above are non-dimensional quantities, details of which are explained in Thomas *et al.*[2] and Balasubramanian and Sujith.[39]

In Eq. (4), K represents the non-dimensional heater power which is defined as,

$$K = \frac{4(\gamma-1)L_w(T_w - \bar{T})}{\gamma M c_0 \bar{p} S\sqrt{3}} \sqrt{\pi\lambda C_v u_0 \bar{\rho} R_w}, \tag{5}$$

where R_w, L_w, T_w are the radius, length, and temperature of the heater wire, respectively, S is the cross sectional area of the duct, $\bar{T}$ is the steady state temperature of the flow. λ and C_v are the thermal conductivity and specific heat at constant volume of the medium within the duct, respectively. The values of all the constants used in this model are the same as in the study by Balasubramanian and Sujith.[39]

In the stochastic term of Eq. (4), σ is the strength of the additive noise and $\epsilon(t)$ is the Gaussian white noise with zero mean and a variance proportional to the square root of the time step used in the computation.[42] We also define a non-dimensional noise intensity given by

$$\beta = \frac{I}{P}, \tag{6}$$

where I is the root mean square value of the applied white noise (calculated from the *rms* of $\sigma\epsilon$ over a period of time) and P is the root mean square value of the acoustic pressure oscillations in the absence of noise.

III. RESULTS AND DISCUSSIONS

In this section, we investigates the effect of noise on the dynamics of a system of two coupled thermoacoustic oscillators. The two types of couplings that we use in this study are time-delay coupling and dissipative coupling. We first show the effect of the external Gaussian white noise added to the time-delay coupled thermoacoustic oscillators on the time evolution of the acoustic pressure signal. We compare this to the noise free case. As can be seen later in this section, a sudden drop in the pressure values at the bifurcation, as observed in the deterministic case, is not perceivable in the presence of noise. Therefore, we use histograms, which show the distribution of pressure amplitudes, to characterize the increasingly smooth bifurcations with the increase in noise intensity.

Furthermore, we show one-parameter bifurcation diagrams, wherein the root mean square value of the pressure signal (p'_{rms}) is plotted against a coupling parameter for different levels of noise intensities, to demonstrate the changes in the nature of bifurcations relative to the deterministic case. The p'_{rms} value is calculated over a long time series (to even out the effect of random perturbations on the calculation) after

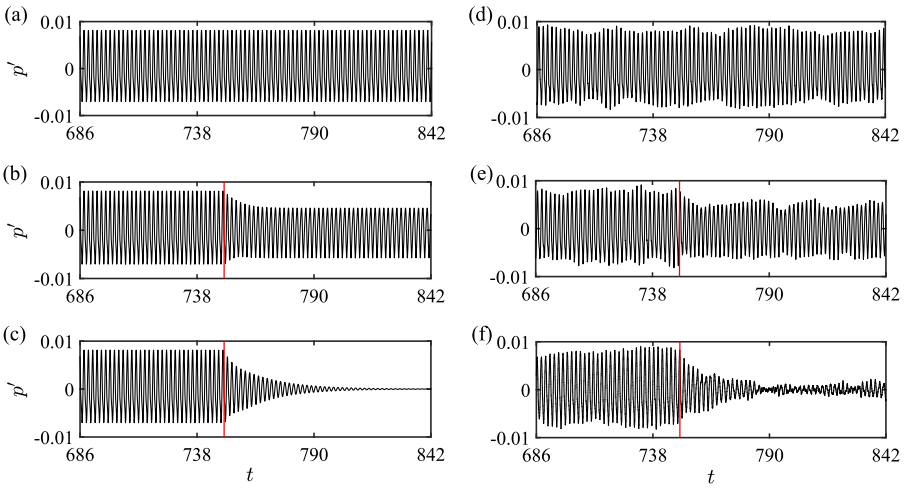

FIG. 1. Temporal variation of non-dimensional acoustic pressure (p') obtained from the thermoacoustic oscillator "a" in the absence of noise [(a), (b), and (c)] and in the presence of noise [(d), (e), and (f)]. (a) In the absence of coupling ($\mathcal{K}_\tau = 0$, $\beta = 0$), (b) in the presence of relatively weak time-delay coupling ($\mathcal{K}_\tau = 0.06$, $\beta = 0$), and (c) in the presence of relatively strong time-delay coupling ($\mathcal{K}_\tau = 0.12$, $\beta = 0$) which can lead to AD state. The corresponding cases in the presence of noise are shown in (d) $\mathcal{K}_\tau = 0$, $\beta = 0.012$, (e) $\mathcal{K}_\tau = 0.06$, $\beta = 0.012$, and (f) $\mathcal{K}_\tau = 0.12$, $\beta = 0.012$. The red vertical line indicates the time instant at which coupling is applied. For all the plots, the non-dimensional heater powers of the two Rijke tubes, $K^a = K^b = 0.8$, $\mathcal{K}_d = 0$, and delay time, $\tau = 0.5$, are fixed.

sufficient time is given for the unsteady pressure oscillations to reach their asymptotic state, post coupling. We also mark the zones of amplitude suppression in two-parameter bifurcation diagrams, where the coupling strength required to achieve a stipulated suppression is plotted as a function of delay time (τ) or detuning ($\Delta\omega$).

A. Effect of time-delay coupling

We start with comparing the time series of acoustic pressure signals obtained in the absence and presence of noise from the system of coupled thermoacoustic oscillators, respectively. We can see that the addition of white noise causes random fluctuations in the amplitude of the signal compared to the deterministic case [Figs. 1(d)–1(f)]. For all the cases in Fig. 1, the non-dimensional heater power value, K, is kept constant at 0.8 ($K_{Hopf} = 0.62$) and the time-delay coupling strength (K_τ) is increased from Figs. 1(a) to 1(c) (without noise) and from Figs. 1(d) to 1(f) (with noise), while K_d is fixed to zero. In Fig. 1, time-delay coupling strength ($\mathcal{K}_\tau$) is the only parameter varied across the three cases of the absence [Figs. 1(a)–1(c)] and the presence [Figs. 1(d)–1(f)] of noise. We observe that there is a decrease in the magnitude of LCO once the coupling is applied in both the cases, as shown in Figs. 1(b) and 1(e). However, when the coupling strength is further increased so as to achieve AD, a complete elimination of oscillations is observed in the noise free case [Fig. 1(c)], while low amplitude aperiodic oscillations persisted in the noisy case [Fig. 1(f)] even after the transition to AD. The dynamics of these aperiodic oscillations observed during the noisy AD state [Fig. 1(f)] are due to the growth of fluctuations of the added noise near the bifurcation point. Further, the amplitude spectrum of such noisy oscillations is broadband with a low amplitude peak near the frequency of LCO.

Since the pressure oscillations do not really die down to zero even with strong coupling in the stochastic case [Figs. 1(d)–1(f)], it is difficult to determine when the transition to AD occurs. Therefore, we make use of histograms

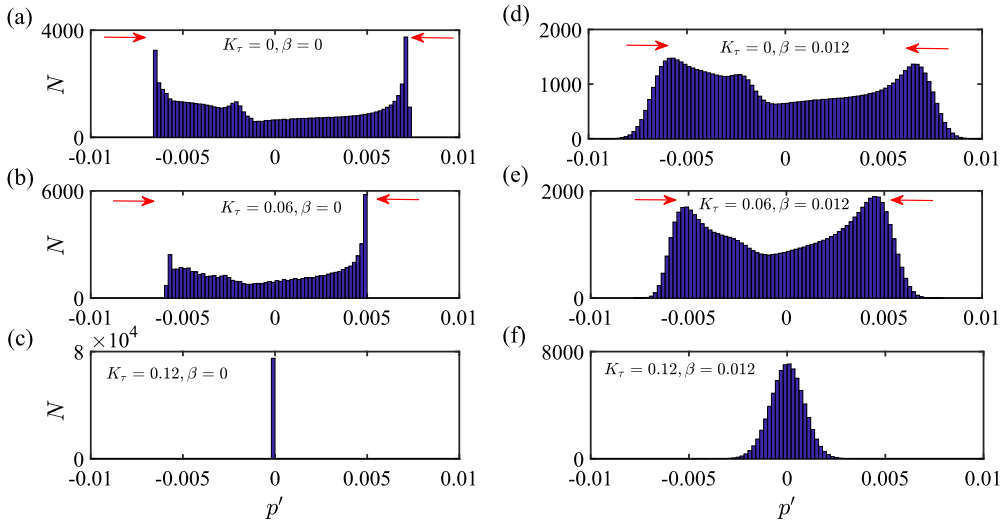

FIG. 2. Histograms plotted for the time series data of acoustic pressure obtained from the thermoacoustic oscillator "a" for the two cases: in the absence of noise [(a), (b), and (c)] and in the presence of noise [(d), (e), and (f)]. ψ^2 represents the variance in the pressure time series. (a) $\mathcal{K}_\tau = 0$, $\beta = 0$, $\psi^2 = 2.164 \times 10^{-5}$; (b) $\mathcal{K}_\tau = 0.06$, $\beta = 0$, $\psi^2 = 1.324 \times 10^{-5}$; (c) $\mathcal{K}_\tau = 0.12$, $\beta = 0$, $\psi^2 = 0$; (d) $\mathcal{K}_\tau = 0$, $\beta = 0.012$, $\psi^2 = 2.215 \times 10^{-5}$; (e) $\mathcal{K}_\tau = 0.06$, $\beta = 0.012$, $\psi^2 = 1.437 \times 10^{-5}$; (f) $\mathcal{K}_\tau = 0.12$, $\beta = 0.012$, $\psi^2 = 7.023 \times 10^{-7}$. The transients in the time series are not included in the data used for plotting histograms. We see that the acoustic pressure amplitude distribution changes from bimodal to unimodal with increasing $\mathcal{K}_\tau$ which can be ascribed to the transition from LCO to AD. The red colored arrows indicate the position of the peaks.

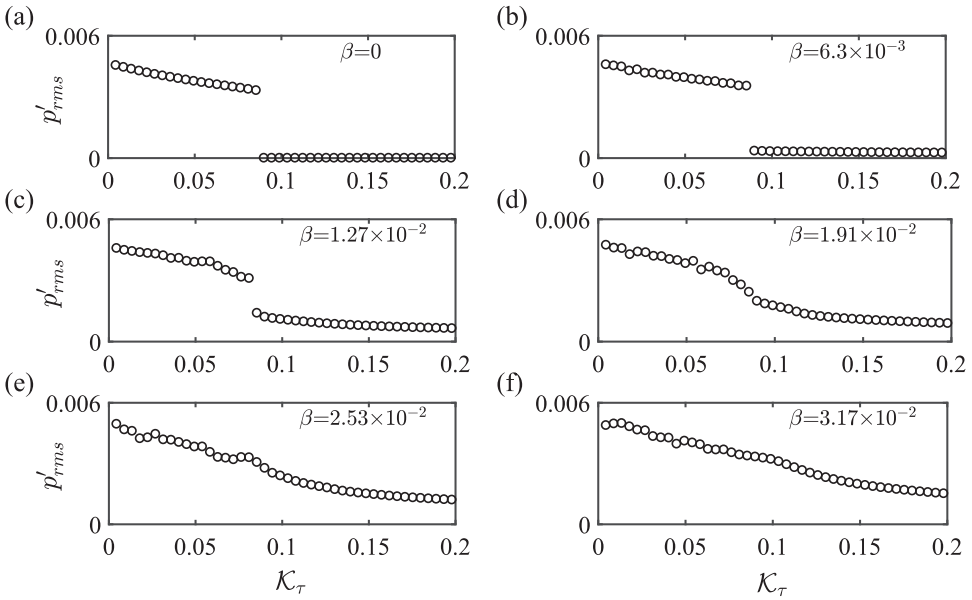

FIG. 3. Bifurcation diagrams depicting the variation of root mean square value of the non-dimensionalized acoustic pressure (p'_{rms}) with time-delay coupling strength ($\mathcal{K}_\tau$) between the two thermoacoustic oscillators for different values of noise intensity, β. (a) $\beta = 0$, (b) $\beta = 6.8 \times 10^{-3}$, (c) $\beta = 1.37 \times 10^{-2}$, (d) $\beta = 2.04 \times 10^{-2}$, (e) $\beta = 2.73 \times 10^{-2}$, and (f) $\beta = 3.41 \times 10^{-2}$. For all the figures, $K^a = K^b = 0.8$, $\mathcal{K}_d = 0$, and $\tau = 0.5$. We observe a departure from the abrupt nature of the transition from LCO to AD with increase in β, due to the amplification of noise after the bifurcation point.

to detect the bifurcations from LCO to AD in the stochastic case. In Fig. 2, we present six histograms corresponding to the six cases presented in Fig. 1. The value on the ordinate, N, represents the number of data points in the pressure time series, p'. We can see that, in the absence of noise, the amplitude distribution of p' is bimodal with two distinct peaks seen away from the mean [Fig. 2(a)], as described in the earlier literature.[42,43] As we introduce a time-delay coupling between the two oscillators, we observe that these two peaks come closer to the mean of the distribution [Fig. 2(b)]. When we further increase $\mathcal{K}_\tau$ to a value greater than $\mathcal{K}_{\tau,critical} = 0.09$ so as to reach the state of AD, we see that pressure distribution essentially exhibits a spiky behaviour at the mean [see Fig. 2(c)], which is zero in this case. On the other hand, when we add external noise to the uncoupled system, we observe that there is a decrease in the height of the peaks as well as an increase in the spread of distribution [Fig. 2(d)]. Also the peaks become broader in the stochastic case in contrast to the sharp peaks observed in the deterministic case. The increase in the spread conforms to increase in the variance (ψ^2) of the pressure time series when the noise is added. Similar to the case of absence of noise, these two peaks in the distribution come closer to the mean when the coupling is introduced in the system, as depicted in Fig. 2(e). With further increase in the $\mathcal{K}_\tau$ value [Fig. 2(f)], we see that the two peaks merge into a single peak. We can characterize this transition in the pressure distribution from bimodal to unimodal as an indicator of the bifurcation to AD in the stochastic case. However, this transition from LCO to AD is a smooth process and hence it is difficult to mention a critical parameter value at which the distribution changes from bimodal to unimodal.[44]

Now, we study the effect of variation in the noise intensity on the one-parameter bifurcation diagram. Figure 3 refers to the case where time-delay coupling alone is applied on a system of two identical ($\omega_b/\omega_a = 1$) thermoacoustic oscillators. We can observe a change in the abrupt nature of the transition with a change in $\mathcal{K}_\tau$, when we increase β, as shown in Figs. 3(a)–3(f). We notice that, when $\beta = 0$, a subcritical Hopf bifurcation happens at a critical $\mathcal{K}_\tau$ value [i.e., the value of $\mathcal{K}_\tau$ at which a sudden drop in the p'_{rms} happens in Fig. 3(a)]. Figure 3(b), where $\beta = 6.8 \times 10^{-3}$, also exhibits a similar behavior although the p'_{rms} values do not reach zero after bifurcation. As we further increase β, the drop in p'_{rms} becomes less abrupt and more smooth, as observed from Figs. 3(c)–3(f),

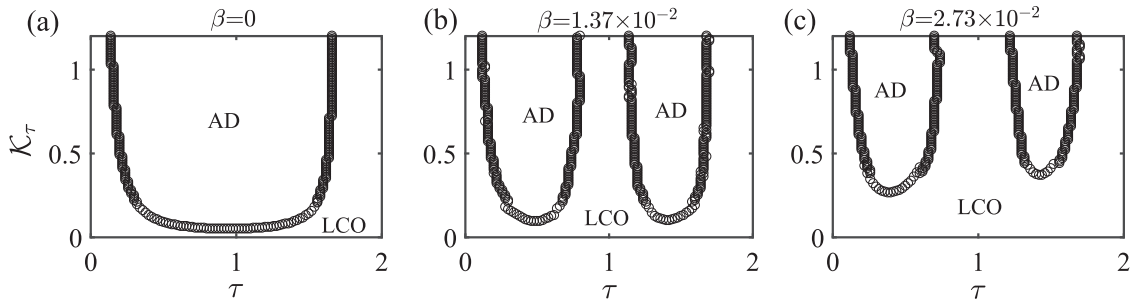

FIG. 4. Two-parameter bifurcation diagram in the parameter plane of time-delay coupling strength ($\mathcal{K}_\tau$) and delay time (τ) for different values of noise intensities: (a) $\beta = 0$, (b) $\beta = 1.37 \times 10^{-2}$, and (c) $\beta = 2.73 \times 10^{-2}$. The markers in (a) correspond to the points in the parameter plane where bifurcation from LCO to AD occurs. In (b) and (c), the markers correspond to the points where the time-delay coupling between the two thermoacoustic oscillators leads to the suppression of LCO amplitude to 20% of its uncoupled value (i.e., when $\mathcal{K}_\tau = 0$). For all the plots, $K^a = K^b = 0.8$, $\mathcal{K}_d = 0$, and $\omega_b/\omega_a = 1$. LCO marked in the plots refers to the stochastic limit cycle oscillations. We observe that, introduction of noise results in a qualitative change as well as a reduction in the size of amplitude suppression zones.

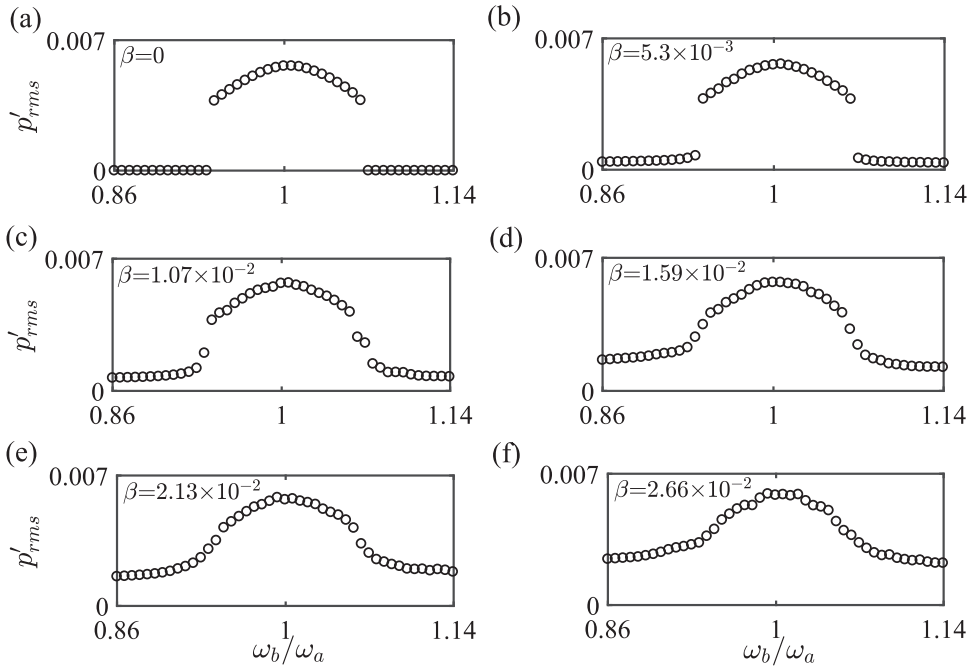

FIG. 5. One-parameter bifurcation diagrams depicting the variation of p'_{rms} with ω_b/ω_a for different values of noise intensity: (a) $\beta = 0$, (b) $\beta = 5.3 \times 10^{-3}$, (c) $\beta = 1.07 \times 10^{-2}$, (d) $\beta = 1.59 \times 10^{-2}$, (e) $\beta = 2.13 \times 10^{-2}$, and (f) $\beta = 2.66 \times 10^{-2}$. Here, $K^a = K^b = 1.02$, $\mathcal{K}_\tau = 0$, and $\mathcal{K}_d = 0.16$. We observe that similar to Fig. 3, the transition from LCO to AD becomes smoother with increasing β.

which is due to the amplification of noise after the bifurcation of LCO to AD. Therefore, in the context of transition to AD, we can say that noise induces a change in the sudden drop of the values of acoustic pressure, as observed for a subcritical Hopf bifurcation in the deterministic case. This behaviour of the amplification of noise after the transition from LCO to AD is similar to the results from earlier studies on the effect of noise on nonlinear oscillator models, which predicted a smoothing effect on the transition from steady state to LCO due to the phenomenon of prebifurcation amplification of noisy fluctuations.[3,42–46] On the contrary, in Fig. 3, we observe the amplification of noise after the bifurcation of LCO to AD. We also observe that, in contrast to the case where noise is absent [Fig. 3(a)], a complete cessation of oscillations as in amplitude death (AD) is not possible in the presence of noise [Figs. 3(b)–3(f)]. Furthermore, from Fig. 3(b) we can see that, with the addition of low amplitude external noise, the bifurcation to AD happens at a lower value of $\mathcal{K}_\tau$ than the noise-free case [Fig. 3(a)]. Such cases where bifurcation happens earlier in the presence of noise is found in the past literature.[44]

Further, we use a two-parameter bifurcation diagram to demonstrate the zones of the maximum suppression achieved through the coupling of two Rijke tube oscillators. Figure 4 is the bifurcation diagram in the parameter plane of time-delay coupling constant ($\mathcal{K}_\tau$) and delay time (τ). The data points in Figs. 4(b) and 4(c) correspond to the points where the amplitude of oscillations in both the Rijke tube oscillators become approximately 20% of their initial uncoupled amplitude. Since the nontrivial response of the thermoacoustic system to noise causes p'_{rms} value to increase to higher amplitudes from the base noise level,[47] we consider "80% reduction in the initial amplitude of LCO" as a good measure of suppression of the oscillatory state in the presence of noise. Here, when the amplitude of oscillations is approximately equal to or lesser than 20% of its initial value, we refer to it as AD state, and when this amplitude value is greater than 20%, we call it as LCO state. This is in contrast with the complete suppression of oscillations to a zero value, as observed in the deterministic case.[2] For the case without noise, we observe a U-shaped plot which is centered around the value of $\omega\tau = \pi$, where $\omega = 3.26$ for both the Rijke tube oscillators in this case [see Fig. 4(a)]. However, this is an ideal scenario and therefore may not be achieved in real systems. As we introduce a small amount of noise into the coupled system, we see that, in the range of $\mathcal{K}_\tau$ and τ values considered, the plot breaks into two independent U-shaped parts centered around the values of $\omega\tau$ equal to $\pi/2$ and $3\pi/2$. As we further increase the noise intensity, we observe an increase in the coupling strength required to attain the 80% reduction in the amplitude of LCO. We also notice an increase in the gap between the two U-shaped regions. Therefore, while aiming for a particular amount of suppression, we need to have an idea about the

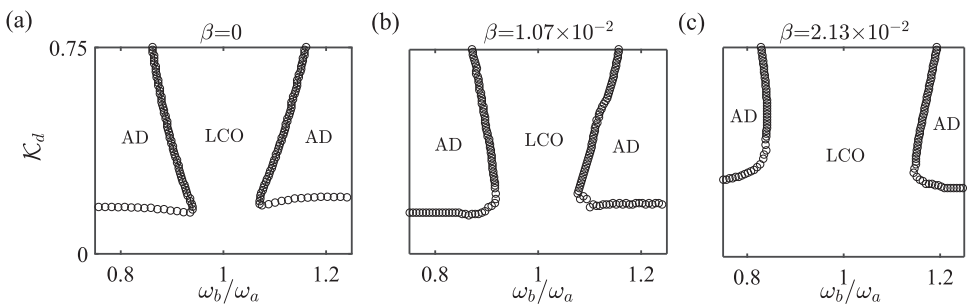

FIG. 6. Two-parameter bifurcation diagram in the parameter plane of dissipative coupling strength ($\mathcal{K}_d$) and ratio of natural frequencies (ω_b/ω_a) of the two coupled thermoacoustic oscillators for different values of noise intensities (for $\mathcal{K}_\tau = 0$): (a) $\beta = 0$, (b) $\beta = 1.07 \times 10^{-2}$, and (c) $\beta = 2.13 \times 10^{-2}$. We observe that with an increase in β, the amplitude of suppression zones becomes smaller in the region considered.

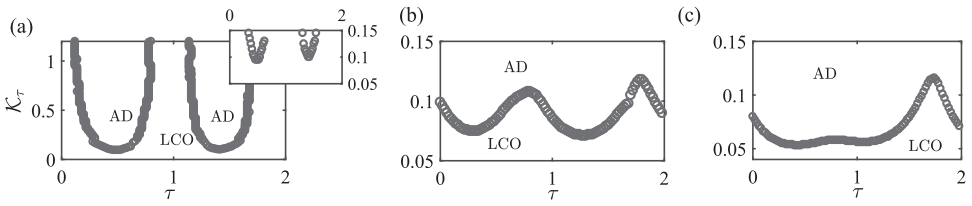

FIG. 7. Two-parameter bifurcation diagram in the parameter plane of time-delay coupling strength ($\mathcal{K}_\tau$) and delay time (τ), when (a) $\omega_b/\omega_a = 1$, $\mathcal{K}_d = 0$; (b) $\omega_b/\omega_a = 0.923$, $\mathcal{K}_d = 0$; (c) $\omega_b/\omega_a = 0.923$, $\mathcal{K}_d = 0.05$. For all the three cases, $\beta = 1.37 \times 10^{-2}$. Note that the ordinates are not the same for all the plots.

intensity of noise prevailing in the system to choose the right values of coupling strength and delay time.

B. Effect of dissipative coupling

We now consider the effect of noise on the one-parameter bifurcation diagram of a dissipatively coupled thermoacoustic systems alone (i.e., $K_\tau = 0$). Since dissipative coupling alone is not capable of achieving AD in a system of two identical ($\omega_b/\omega_a = 1$) oscillators,[48] the two thermoacoustic oscillators considered in this case have non-identical natural frequencies ($\omega_b/\omega_a \neq 1$).

Figure 5 depicts the variation of p'_{rms} with the ratio of natural frequencies of the two thermoacoustic oscillators. From the deterministic case [Fig. 5(a)] we note that, AD is possible with dissipative coupling alone only when there is sufficient detuning between the two thermoacoustic oscillators. We can see that p'_{rms} drops to zero on either side of $\omega_b/\omega_a = 1$, when the transition to AD happens. Similar to Fig. 3, we can observe a change in the abrupt nature of the transition as the noise intensity is increased from Figs. 5(a) to 5(f). We observe that, the sudden drop in the value of p'_{rms} at a critical ω_b/ω_a, as seen in the deterministic case [Fig. 5(a)], now becomes smoother with increase in β. We also see that a complete cessation of oscillation as in amplitude death (AD) is not possible in the presence of noise [Figs. 5(b)–5(f)]. However, a good amount of suppression is achievable with dissipative coupling, when there is sufficient detuning between the two thermoacoustic oscillators.

We further investigate the effect of noise on the two-parameter bifurcation diagram when the dissipative coupling alone is present between two oscillators. Figure 6 is the two-parameter bifurcation diagram produced in the plane of dissipative coupling strength ($\mathcal{K}_d$) and the ratio of natural frequencies (ω_b/ω_a). The markers in Fig. 6 have the same meanings as in Fig. 4. The synchronization characteristics of LCO region for different values of these coupling parameters are elaborately discussed in Thomas *et al.*[2] We see that a significant reduction in the amplitude of pressure fluctuations can be attained in two dissimilar ($\omega_b/\omega_a \neq 1$) thermoacoustic oscillators coupled in the presence of noise ($\beta \neq 0$) by applying the appropriate value of dissipative coupling. The bifurcation diagrams in the two-parameter plane in the presence of noise [Figs. 6(b) and 6(c)] are qualitatively similar to the noise free case [Fig. 6(a)]. The increase in the noise intensity leads to a reduction in the size of the region for which amplitude suppression is observed in the parameter plane. Also, it can be noted that as the value of β is increased from 1.07×10^{-2} in Fig. 6(b) to 2.13×10^{-2} in Fig. 6(c), the plot shifts up and the gap around $\omega_b/\omega_a = 1$ widens. Therefore, we can conclude that higher coupling strength and higher detuning are needed to achieve the same amount of suppression with increased noise levels (β) in the system.

C. Effect of simultaneous application of time-delay and dissipative coupling

Furthermore, we examine the case where both the couplings (time-delay and dissipative) are applied simultaneously[1] on the thermoacoustic oscillators in the presence of noise (Fig. 7). From Fig. 7(b), we note that the introduction of detuning results in the joining of two distinct regions of AD [as seen in Fig. 7(a)], which in turn, causes an increase in the overall region for which 80% suppression (or noisy AD state) is observed in the thermoacoustic oscillations. We also notice a small reduction in the minimum value of K_τ (for example, near τ = 0.5 and 1.5) at which AD is observed in both the oscillators [see inset of Figs. 7(a) and 7(b)]. Further, on the application of a dissipative coupling ($K_d = 0.05$), we observe an additional decrease in the values of K_τ required to achieve 80% amplitude suppression (refer to the region for τ values from 0 to 1.5 in Fig. 7(c). Therefore, we can conclude that the addition of weak dissipative coupling in addition to a finite detuning in the time-delay coupled thermoacoustic oscillators increases the ease of achieving amplitude suppression in noisy case. Similar observations of effectiveness in achieving AD at lower value of coupling parameters from the simultaneous application of time-delay and dissipative couplings have been reported previously by Biwa *et al.*[1] and Thomas *et al.*[2] in the deterministic case.

IV. CONCLUSIONS

In the present study, we numerically investigate the effect of Gaussian white noise on the dynamics of a system of two coupled horizontal Rijke tubes—prototypical thermoacoustic oscillators. We find that, although a complete cessation in the amplitude of limit cycle oscillations (LCO) or amplitude death (AD), as in the deterministic case, is not possible in the presence of noise, coupling is still capable of suppressing the unwanted acoustic pressure oscillations to a great extent. We also observe the relative ease of achieving amplitude suppression through the simultaneous application of both time-delay and dissipative coupling mechanisms on the thermoacoustic systems in the presence of noise. Furthermore, we notice a qualitative change in the amplitude distribution of acoustic pressure oscillations from bimodal to unimodal as the dynamics of oscillators change from LCO to AD. We observe that, with increase in the noise intensity, the abrupt transition from LCO to AD, observed during deterministic case, becomes smoother. We ascribe this smoothening

behaviour of the transition to the phenomenon of noise amplification that happens in the vicinity of bifurcation in the AD state. However, a detailed investigation of this phenomenon of growth in the fluctuations of noise after the transition from LCO to AD in the system of coupled limit cycle oscillators needs further investigation and will be a subject of future study.

ACKNOWLEDGMENTS

This work was supported by Office of Naval Research (Contract Monitor: Dr R. Kolar; Grant No. N62909-18-1-2061).

[1]T. Biwa, S. Tozuka, and T. Yazaki, Phys. Rev. Appl. **3**, 034006 (2015).
[2]N. Thomas, S. Mondal, S. A. Pawar, and R. Sujith, Chaos: Interdiscip. J. Nonlinear Sci. **28**, 033119 (2018).
[3]E. Surovyatkina, Nonlinear Process. Geophys. **12**, 25 (2005).
[4]S. Aumaître, K. Mallick, and F. Pétrélis, J. Stat. Mech.: Theory Exp. **2007**, P07016 (2007).
[5]W. Horsthemke, in *Non-Equilibrium Dynamics in Chemical Systems* (Springer, 1984), pp. 150–160.
[6]P. Kuznetsov, R. Stratonovich, and V. Tikhonov, in *Non-Linear Transformations of Stochastic Processes* (Elsevier, 1965), pp. 223–228.
[7]H.-S. Hahn, A. Nitzan, P. Ortoleva, and J. Ross, Proc. Natl. Acad. Sci. **71**, 4067 (1974).
[8]K. Wiesenfeld, J. Stat. Phys. **38**, 1071 (1985).
[9]P. C. Matthews, and S. H. Strogatz, Phys. Rev. Lett. **65**, 1701 (1990).
[10]A. Pikovsky, M. Rosenblum, and J. Kurths, *Synchronization: A Universal Concept in Nonlinear Sciences* (Cambridge University Press, 2003), Vol. 12.
[11]Y. Kuramoto, Prog. Theor. Phys. Suppl. **79**, 223 (1984).
[12]D. R. Reddy, and A. Sen, Phys. Rev. Lett. **80**, 5109 (1998).
[13]R. Herrero, M. Figueras, J. Rius, F. Pi, and G. Orriols, Phys. Rev. Lett. **84**, 5312 (2000).
[14]R. E. Mirollo, and S. H. Strogatz, J. Stat. Phys. **60**, 245 (1990).
[15]J. W. S. Rayleigh, Nature **18**, 319 (1878).
[16]R. Sujith, M. Juniper, and P. Schmid, Int. J. Spray Combust. Dyn. **8**, 119 (2016).
[17]K. McManus, T. Poinsot, and S. M. Candel, Prog. Energy Combust. Sci. **19**, 1 (1993).
[18]S. C. Fisher, and S. A. Rahman, in *Remembering the Giants: Apollo Rocket Propulsion Development* (NASA Stennis Space Center, 2009).
[19]S. J. Shanbhogue, S. Husain, and T. Lieuwen, Prog. Energy Combust. Sci. **35**, 98 (2009).
[20]A. A. Putnam, *Combustion Driven Oscillations in Industry* (Elsevier Publishing Company, 1971).
[21]S. A. Pawar, A. Seshadri, V. R. Unni, and R. Sujith, J. Fluid Mech. **827**, 664 (2017).
[22]S. Mondal, V. R. Unni, and R. Sujith, J. Fluid Mech. **811**, 659 (2017).
[23]S. A. Pawar, S. Mondal, N. B. George, and R. Sujith, in *2018 AIAA Aerospace Sciences Meeting* (AIAA, 2018), p. 0394.
[24]S. Mondal, S. A. Pawar, and R. Sujith, in *Energy for Propulsion* (Springer, 2018), pp. 125–150.
[25]S. Mondal, S. A. Pawar, and R. Sujith, in *APS Meeting Abstracts* (APS, 2017).
[26]T. Poinsot, Proc. Combust. Inst. **36**, 1 (2017).
[27]M. P. Juniper, and R. I. Sujith, Annu. Rev. Fluid Mech. **50**, 661–689 (2017).
[28]A. Bicen, D. Tse, and J. Whitelaw, Combust. Flame **72**, 175 (1988).
[29]N. A. Kablar, T. Hayakawa, and W. M. Haddad, in *Proceedings of the 2001 American Control Conference, 2001* (IEEE, 2001), Vol. 3, pp. 2468–2473.
[30]P. Langhorne, A. Dowling, and N. Hooper, J. Propul. Power **6**, 324 (1990).
[31]T. Biwa, Y. Sawada, H. Hyodo, and S. Kato, Phys. Rev. Appl. **6**, 044020 (2016).
[32]S. Balusamy, L. K. Li, Z. Han, M. P. Juniper, and S. Hochgreb, Proc. Combust. Inst. **35**, 3229 (2015).
[33]I. C. Waugh, and M. P. Juniper, Int. J. Spray Combust. Dyn. **3**, 225 (2011).
[34]N. Noiray, and B. Schuermans, Int. J. Non-Linear Mech. **50**, 152 (2013).
[35]P. Clavin, J. Kim, and F. Williams, Combust. Sci. Technol. **96**, 61 (1994).
[36]T. C. Lieuwen, and A. Banaszuk, J. Propul. Power **21**, 25 (2005).
[37]I. Waugh, M. Geuß, and M. Juniper, Proc. Combust. Inst. **33**, 2945 (2011).
[38]K. I. Matveev, "Thermoacoustic Instabilities in the Rijke Tube: Experiments and Modeling," Ph.D. thesis (California Institute of Technology, 2003).
[39]K. Balasubramanian, and R. I. Sujith, Phys. Fluids **20**, 044103 (2008).
[40]P. Subramanian, S. Mariappan, R. I. Sujith, and P. Wahi, Int. J. Spray Combust. Dyn. **2**, 325 (2010).
[41]J. Sterling, and E. Zukoski, Combust. Sci. Technol. **77**, 225 (1991).
[42]E. Gopalakrishnan, and R. Sujith, J. Fluid. Mech. **776**, 334 (2015).
[43]E. Gopalakrishnan, J. Tony, E. Sreelekha, and R. Sujith, Phys. Rev. E **94**, 022203 (2016).
[44]A. Juel, A. G. Darbyshire, and T. Mullin, in *Proceedings of the Royal Society of London A: Mathematical, Physical and Engineering Sciences* (The Royal Society, 1997), Vol. 453, pp. 2627–2647.
[45]S. Sastry, and O. Hijab, Syst. Control. Lett. **1**, 159 (1981).
[46]A. Zakharova, T. Vadivasova, V. Anishchenko, A. Koseska, and J. Kurths, Phys. Rev. E **81**, 011106 (2010).
[47]L. Kabiraj, R. Steinert, A. Saurabh, and C. O. Paschereit, Phys. Rev. E **92**, 042909 (2015).
[48]D. G. Aronson, G. B. Ermentrout, and N. Kopell, Phys. D: Nonlinear Phenom. **41**, 403 (1990).